Rare Metal Materials and Engineering
Volume 54, Issue 12, December 2025
Available online at www.rmme.ac.cn

Science Press

Cite this article as: Bai Run, Huang Li, Liu Hui, et al. High-Temperature Mechanical Properties of TaWHf Alloy Doped with Re and C[J]. Rare Metal Materials and Engineering, 2025, 54(12): 2985-2992. DOI: https://doi.org/10.12442/j.issn.1002-185X.20250168.

ARTICLE

High-Temperature Mechanical Properties of TaWHf Alloy Doped with Re and C

Bai Run[1,2], Huang Li[2], Liu Hui[2], Wang Feng[2], Cai Xiaomei[2], Xia Mingxing[2], Sun Rui[2], Bai Wei[2], Hu Ping[1], Zhang Wen[2]

[1] School of Metallurgy Engineering, Xi'an University of Architecture and Technology, Xi'an, 710055, China; [2] Northwest Institute for Nonferrous Metal Research, Xi'an 710016, China

Abstract: The high-temperature mechanical properties of Ta-8W-2Hf alloy doped with Re (1wt%) and C (0.01wt%) were investigated at room temperature, 1300 °C, and 1500 °C. Results show that fine and dispersed precipitates Ta_2C are detected in crystallized TaWHfReC alloy, which significantly enhance mechanical properties of the alloy. The strength of TaWHfReC alloy is much higher than that of TaWHf alloy, especially at 1300 and 1500 °C. At 1300 °C, the ultimate tensile strength of the TaWHf alloy is 322 MPa, while that of the TaWHfReC alloy reaches 392 MPa. When the temperature rises to 1500 °C, precipitated-phase strengthening remains effective in the TaWHfReC alloy, achieving an ultimate tensile strength of 268 MPa. Additionally, at 1300 °C, the elongation of the TaWHfReC alloy reaches 23.5%, which is nearly twice of that of the TaWHf alloy. The significant improvement in the mechanical properties of the TaWHfReC alloy at elevated temperatures is primarily attributed to the interaction between dislocations and the fine Ta_2C precipitated phase. The fine and uniformly distributed particles effectively inhibit dislocation motion and exhibit a pronounced strengthening effect at high temperatures.

Key words: Ta alloy; solid solution strengthening; precipitated-phase strengthening; mechanical properties; high temperature

1 Introduction

Tantalum alloys are highly valued in industries such as chemical processing, aerospace, and atomic energy due to their exceptional properties, including high melting points, superior strength, good plasticity, corrosion resistance, and outstanding processing performance[1–3]. These characteristics make them ideal for demanding applications, where materials must withstand extreme conditions. However, pure tantalum suffers from relatively low strength, which restricts its use in high-stress environments. To address this issue, various strengthening methods have been developed, with solid solution strengthening and precipitation strengthening being the most prominent[4–5]. These techniques enhance the mechanical properties of tantalum alloys, making them suitable for a wider range of applications.

One of the most common alloying elements in tantalum alloys is tungsten, primarily due to its similar crystalline structures, which facilitate the formation of stable solid solution[6]. Nemat-Nasser et al[7] studied the effect of tungsten content on dynamic crack initiation in Ta, Ta-0.5W, and Ta-12W alloys. They indicated that increasing W content promotes the nucleation and growth of defects. As a result, the tungsten content in tantalum alloys is typically limited to 12wt% to balance strength and ductility[8]. In addition to tungsten, other refractory elements such as niobium[9–10], rhenium[11–12], hafnium[13], are often incorporated into tantalum alloys to enhance strength, ductility, and comprehensive properties, including good welding performance, corrosion resistance, and high-temperature creep resistance.

Except for solid solution strengthening, Ta alloy can also be strengthened by introducing precipitates or secondary-phase

Received date: April 01, 2025
Foundation item: Supported by Shaanxi Provincial Department of Science and Technology (2024GX-YBXM-362); Supported by Northwest Institute for Nonferrous Metal Research (070YC2314); Key R&D Plan of Shaanxi Province (2024QCYKXJ-116); Scientific and Technological Innovation Team Project of Shaanxi Innovation Capability Support Plan of China (2022TD-30)
Corresponding author: Hu Ping, Ph. D., Professor, School of Metallurgy Engineering, Xi'an University of Architecture and Technology, Xi'an 710055, P. R. China, E-mail: huping1985@126.com

particles, such as carbide and nitrogen[14–15]. Ta_2C shows significant plastic deformation at high temperature[16]. Leon et al[17] confirmed that pyramidal dislocation slip of the $a/3 <11\bar{2}3>\{10\bar{1}1\}$ can be activated to improve plasticity.

The combination of high strength and moderate fracture toughness makes TaWHf alloys particularly attractive for advanced applications, such as space nuclear reactor power sources[18–19]. These alloys take advantage of the high melting points of their constituent elements. Hafnium has a melting point of 2222 °C, which is still significantly lower than the melting point of Ta. However, the volatility of hafnium under high-temperature vacuum conditions poses a challenge to alloy stability[20]. The composition and homogeneity of these alloys play a critical role in determining their properties. For instance, two well-known tantalum alloys, T-111 (Ta-8%W-2%Hf)[21] and ASTAR-811C (Ta-8%W-1%Re-1%Hf-0.025%C)[22], were extensively studied in the 1960s and 1970s for their superior high-temperature creep strength and fabricability. Despite the fact that the properties of these alloys have been verified, detailed studies on the microstructure evolution with time under high-temperature conditions remain scarce.

To address these issues, this research focuses on modifying TaWHf alloys by adding rhenium and carbon. Rhenium is known for its ability to enhance high-temperature strength and stability, while carbon can form carbides that contribute to precipitation strengthening[23]. By studying the effects of these additions, this work aims to improve the mechanical properties and microstructural stability of TaWHf alloys, providing valuable insights for their use in extreme environments. The findings will contribute to the development of advanced materials meeting the demands of next-generation aerospace and nuclear applications.

2 Experiment

The TaWHf alloy used in this work was prepared using pure Ta (99.95wt%), pure W (99.95wt%), pure Hf (99.90wt%), and pure Re (99.90wt%) powders. A certain amount of C in the form of graphite powder was added to achieve tantalum carbide in the alloy.

The alloys were produced by high temperature vacuum sintering combined with vacuum electron beam melting. The ingots were remelted three times to promote homogeneity, followed by forging the ingot to Φ50 mm in size. Finally, the bar was extruded and forged to Φ12 mm in size. The composition of the alloy was tested using inductivity coupled plasma-atomic emission spectroscope (ICP-AES).

The tensile samples were obtained from the rolled rod after recrystallization treatment. The geometrical parameter and test standard of samples were according to GB/T 228.1-2010 and GB/T 228.2-2015 at room temperature (RT) and high temperature, respectively. The tensile tests were conducted along the forging direction, and the high-temperature tensile test was conducted at 1300 and 1500 °C under vacuum atmosphere. TaWHf alloys are designed to work for nuclear reactors. The highest working temperature is nearly 1500 °C. In addition, the precipitates Ta_2C are thermally stable at temperatures lower than approximately 1527 °C. Thus, 1300 and 1500 °C were chosen in this research to evaluate the mechanical properties.

The structure of TaWHf alloys was characterized using X-ray diffractometer (XRD, Smartlab SE, Japan) with a Cu target and a scanning angle (2θ) from 20° to 90°. The microstructure of these alloys was analyzed by an optical microscope (OM, OLYMPUS PMG3), a scanning electron microscope (SEM, JSM-6460) equipped with an energy-dispersive spectrometer (EDS), and a transmission electron microscope (TEM, JEM-200CX).

3 Results and Discussion

3.1 Microstructure of TaWHf alloy

Fig.1a–1d show the morphologies of the as-received Ta, W, Hf, and Re powders before mixing. Fine and uniformly sized powders were used for the preparation of designed TaWHf and TaWHfReC alloys. The powder mixing process was conducted in a V-mixer for 24 h to ensure homogeneous distribution. Subsequently, the mixed powders were compacted and vacuum-dried to form sintered billets, which were then subjected to vacuum electron beam melting. The mixed powder morphologies of TaWHf and TaWHfReC alloys are presented in Fig. 1e and Fig. 1i, respectively. EDS elemental distribution mappings of TaWHf are shown in Fig. 1f – 1h, demonstrating relatively uniform distribution of elements in the matrix after 24 h of mixing. Similarly, EDS elemental distribution mappings for TaWHfReC are displayed in Fig.1j–1l. Notably, the bright spots observed in Fig.1l indicate that Hf powder exhibits greater resistance to fragmentation compared to Ta and W powders during the mixing process.

Table 1 presents the chemical composition of TaWHf and TaWHfReC alloys prepared by vacuum electron beam melting. The TaWHf alloy (denoted as 1#) and TaWHfReC alloy (denoted as 2#) exhibit comparable W (7.9wt%) and Hf (1.7wt%) contents. The measured concentration of Re (about 0.9wt%) and C (about 0.01wt%) of TaWHfReC alloys is in good agreement with the designed composition. The compositional analysis reveals minimal variations across different regions of the ingots, indicating a homogeneous distribution of constituent elements throughout the materials.

The forged bars were subjected to annealing treatments at 1400, 1450, and 1550 °C. Through microstructural analysis, the recrystallization temperatures were determined to be 1550 °C for the TaWHf alloy and 1450 °C for the TaWHfReC alloy. Fig.2 shows XRD patterns of the recrystallized TaWHf and TaWHfReC alloys, with pure Ta as a reference. XRD analysis reveals no detectable secondary phases in both alloys. XRD patterns demonstrate that both alloys maintain a single body-centered cubic (bcc) solid-solution structure, which is consistent with the crystal structure of pure tantalum.

Fig.3 presents OM images of the recrystallized TaWHf and TaWHfReC alloys. Both alloys exhibit equiaxed grains after the annealing process. However, a distinct difference in grain morphology is observed between the two alloys. The

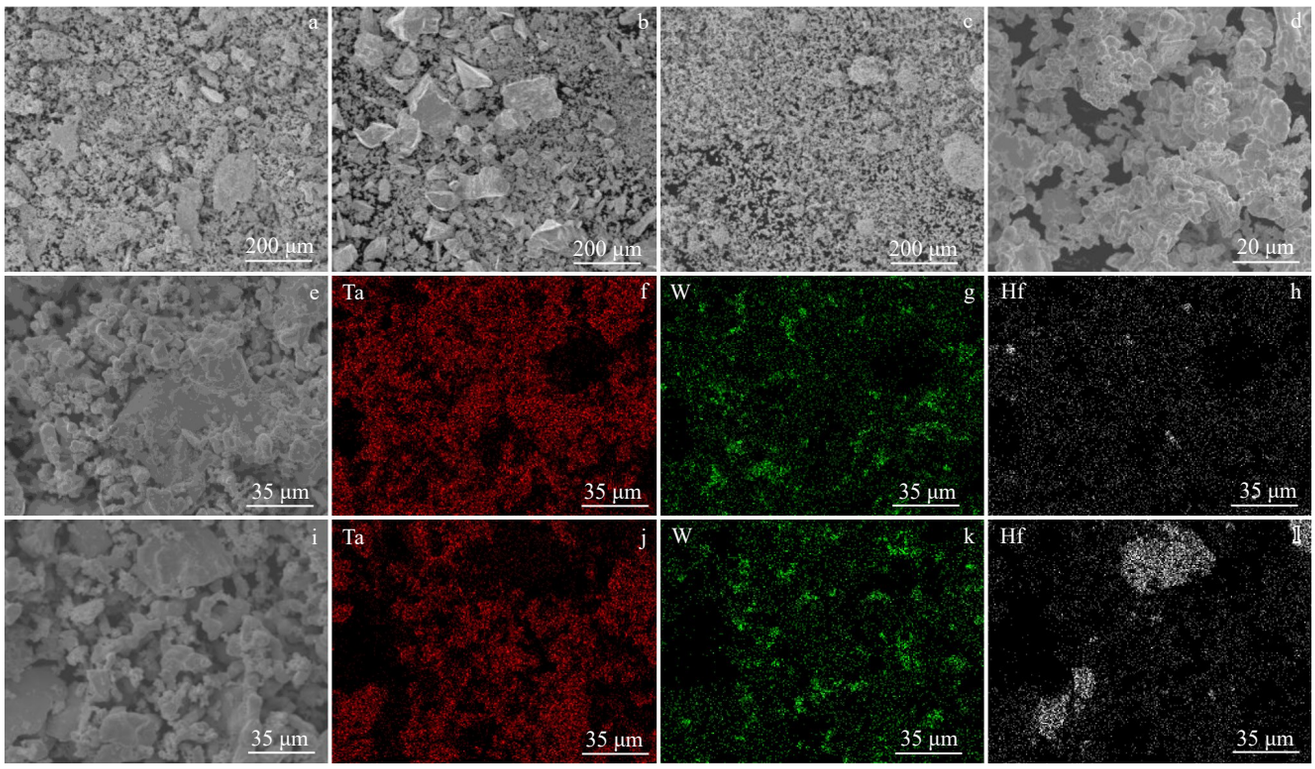

Fig.1 SEM images for raw Ta (a), Hf (b), W (c), and Re (d) powder; SEM images (e, i) and corresponding EDS elemental distribution mappings (f–h, j–l) of TaWHf powders (e–h) and TaWHfReC powders (i–l) after mixing for 24 h

Table 1 Chemical composition of TaWHf and TaWHfReC alloys

Sample	Location	W	Hf	Re	C	N	O	H	Ta
1#	Upper	7.92	1.67	-	0.003	0.006	0.008	0.006	Bal.
	Middle	7.85	1.69	-	0.002	0.005	0.006	0.005	Bal.
2#	Upper	7.89	1.77	0.92	0.015	0.001	0.022	0.008	Bal.
	Middle	7.90	1.68	0.91	0.013	0.001	0.011	0.008	Bal.

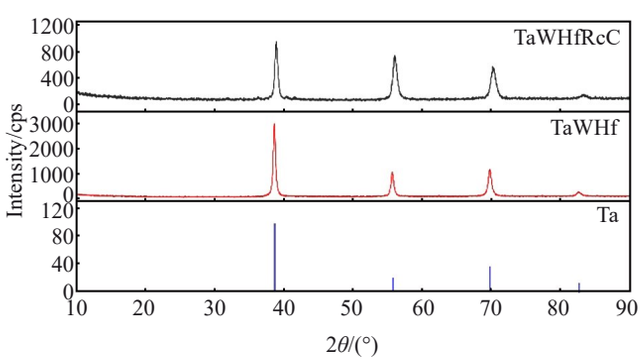

Fig.2 XRD patterns of pure Ta, TaWHf alloy, and TaWHfReC alloy

TaWHfReC alloy has significantly finer and more uniform grains compared to the TaWHf alloy. Under identical deformation conditions, the recrystallization temperature of the TaWHfReC alloy is approximately 100 °C lower than that of the TaWHf alloy. Furthermore, quantitative analysis reveals that the average grain size of the TaWHfReC alloy is nearly half of that of the TaWHf alloy. This remarkable grain refinement of the TaWHfReC alloy can be attributed to the strong grain-boundary pinning effect induced by the addition of elements Re and C.

Fig. 4 shows SEM images of the recrystallized alloys, revealing distinct microstructural characteristics. In the TaWHfReC alloy, fine particles are distributed throughout the matrix, with the majority located within the grains and a smaller fraction situated along the grain boundaries. These particles are identified as secondary phase precipitates. As indicated in Fig. 4d, the secondary phase particles at the grain boundaries exhibit significantly larger dimensions compared to those within the grains. Moreover, the grain boundary precipitates demonstrate a characteristic ellipsoidal morphology. In contrast, the TaWHf alloy shows a markedly different microstructure. There is no detectable secondary phase particles, either within the grains or at the grain boundaries.

Fig. 5 presents TEM images of the recrystallized TaWHf alloy, illustrating its microstructural characteristics. As demonstrated in Fig. 5a – 5b, the dislocation density is significantly reduced, which can be attributed to the completion of the recrystallization process. However, a small number of dislocations and dislocation outcrops are still visible within the grains. The selected area electron diffraction (SAED) patterns, shown in Fig. 5c – 5d, were acquired along the [011] and [012] zone axes, respectively. These diffraction patterns confirm the presence of a single bcc solid-solution phase. Importantly, the absence of streaking or superlattice reflections in the diffraction patterns further indicates that there is no phase decomposition during the annealing process.

TEM images of the TaWHfReC alloy after annealing at

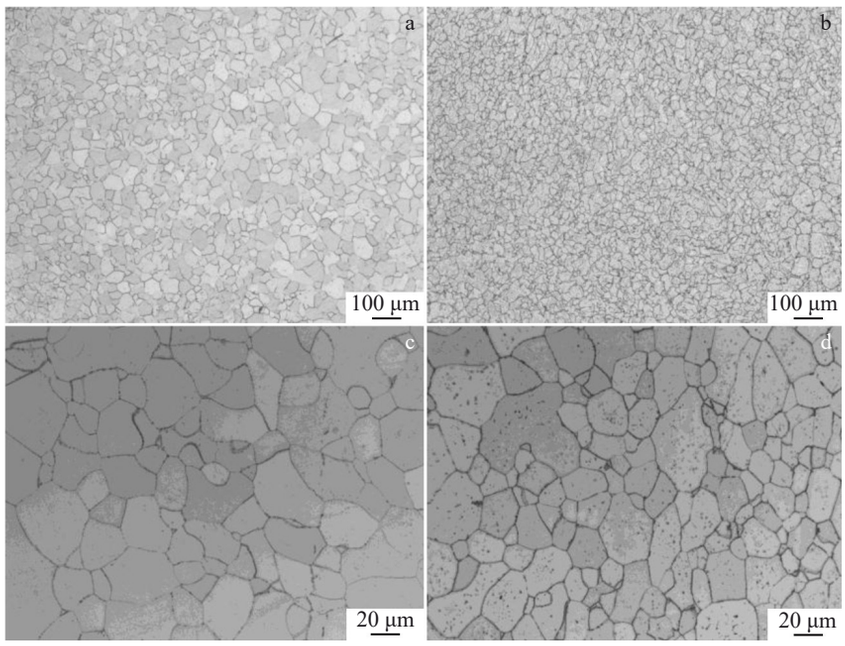

Fig.3 OM images of TaWHf alloy after heat treatment at 1550 °C for 1 h (a, c) and TaWHfReC alloy after heat treatment at 1450 °C for 1 h (b, d)

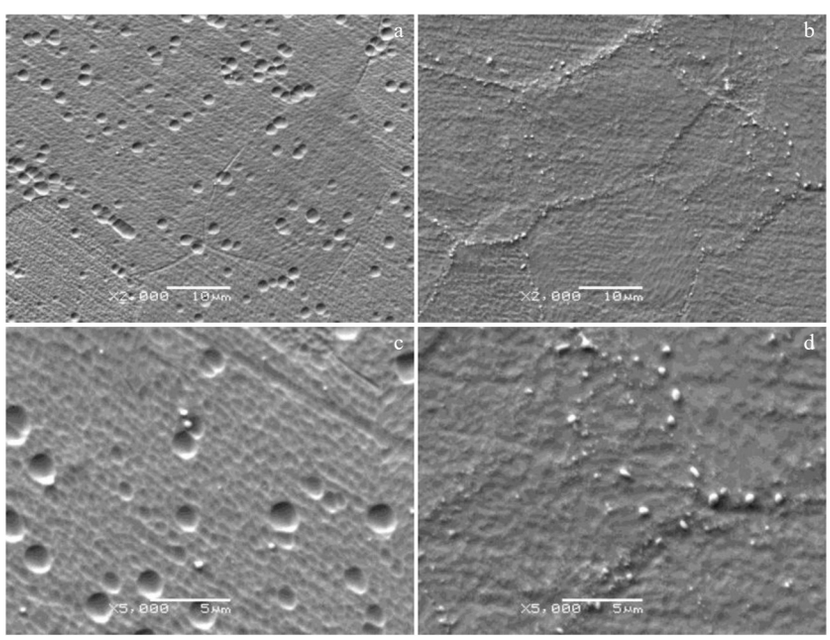

Fig.4 SEM images of recrystallized TaWHf alloy (a, c) and TaWHfReC alloy (b, d)

1450 °C for 1 h are shown in Fig. 6. The micrographs clearly demonstrate the presence of secondary phase particles distributed within the grains and along the grain boundaries. As shown in Fig. 6a, over 90% of these particles exhibit a rounded or spherical morphology. SAED pattern in Fig. 6b displays two distinct sets of diffraction spots, indicated by yellow and green arrows. The yellow arrows correspond to the [001] zone axis of the matrix phase, while the green arrows represent the diffraction pattern of the secondary phase, which is identified as Ta_2C with hexagonal close-packed structure along the $[01\bar{1}1]$ zone axis. Furthermore, the crystallographic orientation relationship between the matrix and precipitates is the $[\bar{1}10]$ in matrix parallel to $[\bar{1}011]$ in Ta_2C. The diffraction pattern of TaWHfReC alloy, which is consistent with that of TaWHf alloy, is identified as a bcc Ta structure.

Fig. 6c shows dark field image that is corresponding to Fig. 6a. SAED pattern along $[\bar{1}101]$ zone axis is shown in Fig. 6c. The light points in Fig. 6c are all Ta_2C particles. Fine and dispersed precipitations in TaWHfReC alloy can suppress the extension of dislocations, as shown in Fig. 6d, leading to the excellent mechanical properties at high temperatures. Based on the Ta-C phase diagram, Ta_2C is quite stable at

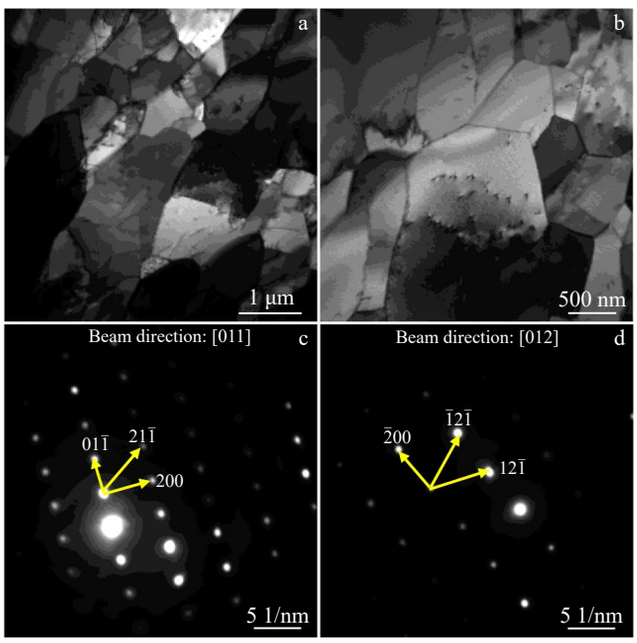

Fig. 5 TEM bright field images (a–b) and SAED patterns along the beam direction of [011] (c) and [012] (d) of recrystallized TaWHf alloy

temperature lower than 1527 °C[14].

3.2 Mechanical properties of TaWHf and TaWHfReC alloys

Tensile tests were conducted at RT, 1300 °C, and 1500 °C to evaluate the mechanical properties of TaWHf and TaWHfReC alloys. While the RT tensile tests were performed in air, the elevated temperature tensile tests were conducted under a vacuum condition maintained at $\leqslant 2.5\times10^{-2}$ Pa to prevent oxidation. The tensile properties, including yield strength (YS), ultimate tensile strength (UTS), and elongation (EL), are summarized in Table 2.

The results in Table 2 reveal that the TaWHfReC alloy exhibits a significant strengthening effect. UTS of TaWHfReC alloy is approximately 50 MPa higher than that of the TaWHf alloy at both RT and 1500 °C. This indicates that the strengthening mechanism becomes more pronounced at elevated temperatures. In terms of ductility, a general decreasing trend is observed as the testing temperature increases to 1300 °C. At 1300 °C, UTS increases from 322 MPa in TaWHf alloy to 392 MPa in TaWHfReC alloy, while EL rises from 12.0% (TaWHf alloy) to 23.5% (TaWHfReC alloy). EL of the TaWHfReC alloy is nearly twice of that of the TaWHf alloy. Remarkably, the TaWHfReC alloy retains an EL of 25% even at 1500 °C. These findings clearly demonstrate that the addition of secondary phase precipitates effectively enhances the high-temperature mechanical properties of the alloy.

As shown in Fig.7, both UTS and YS are decreased with the increase in temperature, which is similar to the results at RT. With the addition of the Re and C into TaWHf alloy, UTS and YS increase at high temperature. After adding both Re and C, UTS and YS increase by a maximum of 70 and 30 MPa at 1300 °C, respectively. And UTS and YS increase by 55 and 20 MPa at 1500 °C, respectively. EL decreases slightly at RT but

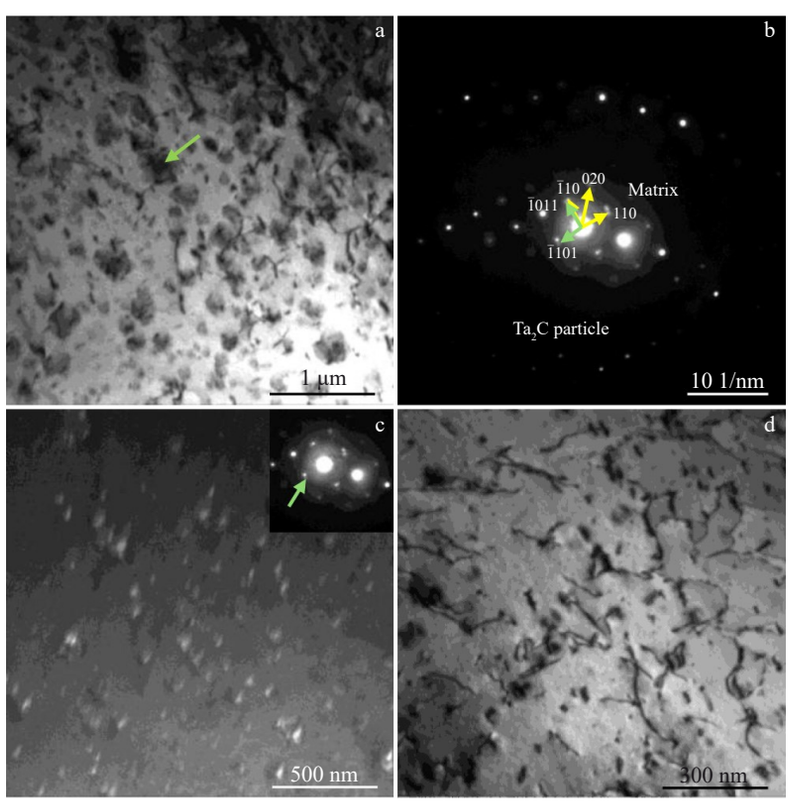

Fig.6 TEM analysis of recrystallized TaWHfReC alloy: (a, d) bright field images; (b) SAED pattern; (c) dark field image with SAED pattern

Table 2 Tensile properties of TaWHf and TaWHfReC alloys

Sample	Test temperature/°C	UTS/MPa	YS/MPa	EL/%
1#	25 (RT)	622	517	40.5
2#	25 (RT)	674	567	31.5
1#	1300	322	243	12.0
2#	1300	392	274	23.5
1#	1500	213	196	21.0
2#	1500	268	218	25.0

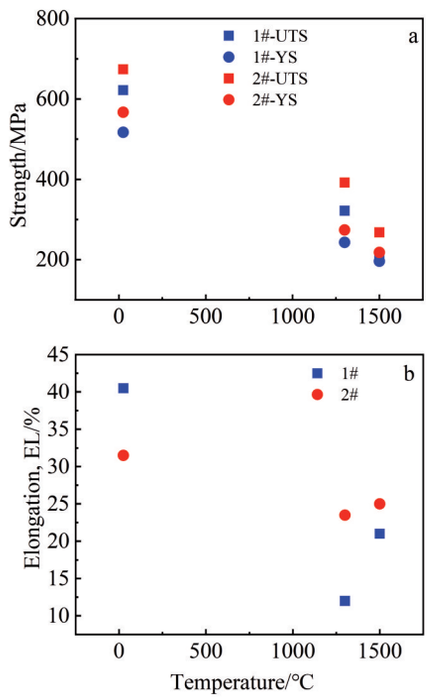

Fig.7 Tensile properties of TaWHf alloy and TaWHfReC alloy at different temperatures: (a) UTS and YS; (b) EL

significantly increases at high temperature.

Fig. 8 shows the fracture morphologies of both alloys after the tensile tests at RT, which show typical cup cone fracture with equiaxed dimples, as shown in Fig. 8a and Fig. 8c. The dimples in TaWHf alloy are large and flat, and many holes are observed in TaWHfReC alloy. The dimple in TaWHfReC alloy is deep. Because the grains of TaWHfReC alloy are finer than that of TaWHf alloy, and many small holes are left in TaWHfReC alloy after the secondary phase particles are pulled out, as shown in Fig.8d.

Fig. 9 shows the microstructure evolution of TaWHfReC alloy after tensile test at 1300 °C to investigate the reasons for the good mechanical properties. An array of precipitations is detected along the grain boundaries, as shown in Fig. 9a and 9c. The interaction between dislocations and the particles are shown in Fig. 9b and 9d. Ta_2C acts as an effective suppression on the extension of dislocation, providing high strength at high temperature. In addition, dislocation arrangements in TaWHfReC alloy are complex, as shown in Fig. 9e–9h. Different $\vec{g}$ ([01$\bar{1}$], [200], and [21$\bar{1}$]) are used to observe the dislocation waves in Fig. 9e. Three groups of dislocations are visible in one $\vec{g}$ but invisible in another $\vec{g}$. According to the dislocation invisible criterion, $\vec{b}$ in Fig. 9g is 1/2[$\bar{1}$1$\bar{1}$], and it is 1/2[111] in Fig.9h.

It is well known that the atomic size of carbon is far lesser than that of Ta[24]. So, carbon occupies interstitial sites and makes the interstitial solid solution during the formation of Ta_2C. The dislocation movement is effectively impeded to improve the tensile properties of the alloy. Dislocation slip is obstructed by the precipitates, and slip bands are bended and twisted, forming a large number of sub-grains. In addition, the grain is refined after adding Re and C. Based on the Hall-Petch formula, the strength is enhanced as grain size

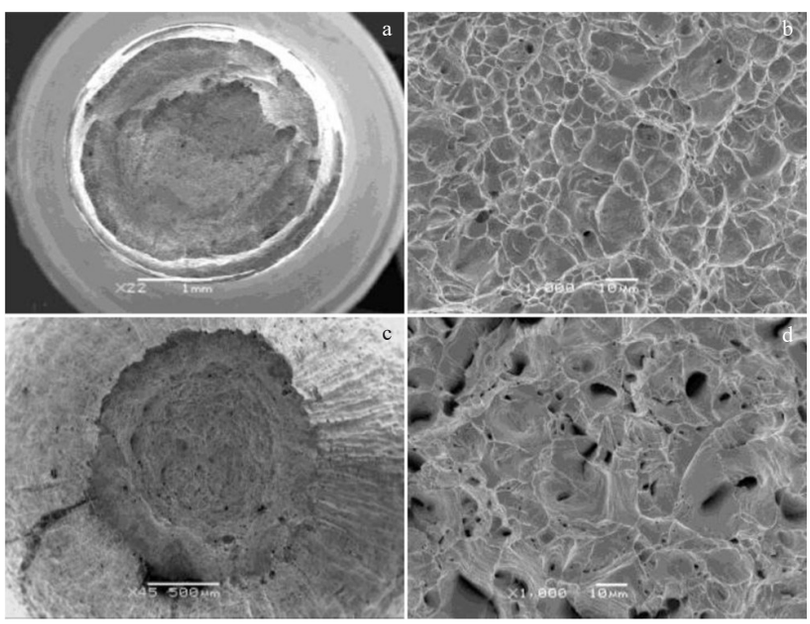

Fig.8 Tensile fracture morphologies of TaWHf alloy (a–b) and TaWHfReC alloy (c–d)

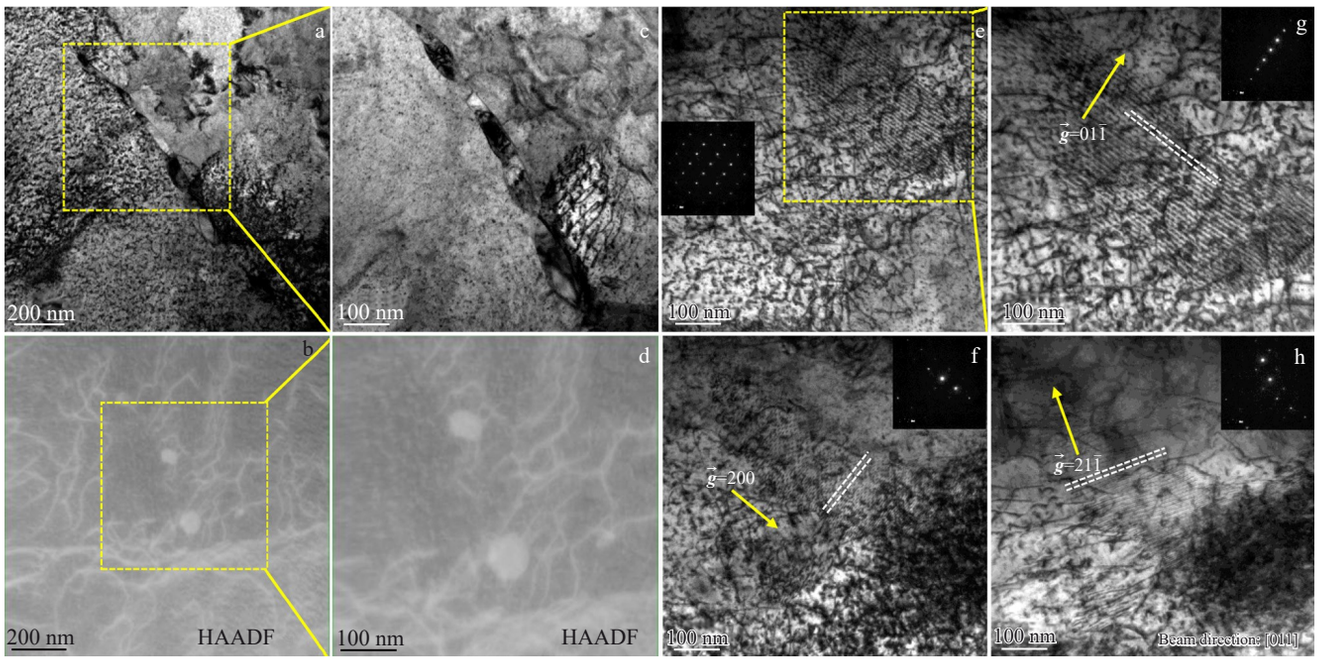

Fig.9 TEM images of TaWHfReC alloy after tensile test at 1300 °C: (a–d) dislocation between secondary phase particles; (e–h) dislocation arrangements with SAED patterns (HAADF means high angle annular dark field)

decreases.

It can be concluded that the improvement of mechanical properties at high temperature with Ta_2C addition is contributed to grain refinement. Fine grains hinder the generation and propagation of cracks. The deflection and branching of the cracks also disperse the stress, which completely offsets the reduction of ductility caused by the addition of brittle Ta_2C. Therefore, the TaWHfReC alloy has better comprehensive properties after Ta_2C strengthening.

4 Conclusions

1) At 1300 °C, UTS increases from 322 MPa in TaWHf alloy to 392 MPa in TaWHfReC alloy, while EL rises from 12.0% (TaWHf alloy) to 23.5% (TaWHfReC alloy). This trend is maintained even at elevated temperatures of 1500 °C.

2) After the addition of Re and C, the recrystallization temperature of the TaWHfReC alloy decreases from 1550 °C to 1450 °C, and the grain size is significantly refined. The average grain size of the TaWHfReC alloy is approximately half of that of the TaWHf alloy.

3) Fine Ta_2C precipitates are formed in the TaWHfReC alloy, which are uniformly distributed within the grains and along the grain boundaries, effectively suppressing dislocation movement and thereby enhancing the high-temperature strength.

References

1 Kim Y M, Kim E P, Noh J W *et al*. *International Journal of Refractory Metals and Hard Materials*[J], 2015, 48: 211

2 Cheng C, Fu Y Q, Du C X *et al*. *International Journal of Refractory Metals and Hard Materials*[J], 2022, 107: 105873

3 Wang Zheng, Yuan Yue, Arshad Kameel *et al*. *Fusion Engineering and Design*[J], 2017, 125: 496

4 Stelmakh V, Rinnerbauer V, Geil R D *et al*. *Applied Physics Letters*[J], 2013, 103: 123903

5 Massey C P, Goetz C K, Lin Y R *et al*. *Journal of Nuclear Materials*[J], 2024, 591: 154906

6 Muzyk M, Nguyen-Manh D, Wróbel J *et al*. *Journal of Nuclear Materials*[J], 2013, 442: 680

7 Nemat-Nasser S, Kapoor R. *International Journal of Plasticity*[J], 2001, 17(10): 1351

8 Gao Fei, Zhang Xianfeng, Serjouei Ahmad *et al*. *Rare Metal Materials and Engineering*[J], 2017, 46(10): 2753

9 Fedorayev I I, Kerimov E Y, Leonov A V *et al*. *International Journal of Refractory Metals and Hard Materials*[J], 2024, 121: 106630

10 El-Genk S, Tournier J M. *Journal of Nuclear Materials*[J], 2005, 340(1): 93

11 Leonard K J, Busby J T, Zinkle S J *et al*. *Journal of Nuclear Materials*[J], 2007, 366(3): 353

12 Gao Xiaoyong, Zhang Lifeng. *Materials Characterization*[J], 2024, 211: 113918

13 He H T, Fang J X, Yang Z *et al*. *Materials Science and Engineering A*[J], 2024, 915: 147217

14 Cotton Dominique, Jacquet Philippe, Faure Sébastien *et al*. *Materials Chemistry and Physics*[J], 2022, 278: 125632

15 Liu Xingliang, Dai Yu, Wang Zhuojian *et al*. *New Carbon Materials*[J], 2021, 36: 1049

16 Wang B, Leon N D, Weinberger C R *et al*. *Acta Materialia*[J], 2013, 61: 3914

17 Leon N D, Wang B, Weinberger C R *et al*. *Acta Materialia*[J],

2013, 61: 3905
18 Tong Yonggang, Peng Xinliang, Liang Xiubing *et al*. *Journal of Alloys and Compounds*[J], 2024, 997: 174955
19 David D J, Snide J A, Moddeman W E. *Applications of Surface Science*[J], 1982, 13: 329
20 Musari A A. *Solid State Sciences*[J], 2021, 122: 106755
21 Sheffler K D, Sawyer J C, Steigerwald E. *Mechanical Behavior of Tantalum-Base T-111 Alloy at Elevated Temperature*[M]. Washington: NASA, 1969
22 Buckman R W, Goodspeed R C. *Precipitation Strengthened Tantalum Base Alloys*[R]. Washington: NASA, 1971
23 Li Xu, Zhang Zhibin, He Pengfei *et al*. *Rare Metal Materials and Engineering*[J], 2023, 52(3): 1131 (in Chinese)
24 Zheng Yongfeng, Hu Xiaofeng, Yang Zhirong *et al*. *Rare Metal Materials and Engineering*[J], 2025, 54(5): 1217 (in Chinese)

Re和C掺杂TaWHf合金的高温力学性能

白　润[1,2]，黄　丽[2]，刘　辉[2]，王　峰[2]，蔡小梅[2]，夏明星[2]，孙　锐[2]，白　伟[2]，胡　平[1]，张　文[2]
(1. 西安建筑科技大学 冶金工程学院，陕西 西安 710055)
(2. 西北有色金属研究院，陕西 西安 710016)

摘　要：研究了掺杂Re (1wt%)和C (0.01wt%)的Ta-8W-2Hf合金在室温、1300 ℃和1500 ℃下的高温力学性能。结果表明，再结晶后的TaWHfReC合金中含有细小的弥散析出相Ta_2C，显著提高了合金的力学性能。在1300和1500 ℃的高温下，TaWHfReC合金的强度远高于TaWHf合金。在1300 ℃时，TaWHf合金的抗拉伸强度为322 MPa，而TaWHfReC合金的抗拉伸强度达到了392 MPa。当温度升至1500 ℃时，析出相强化在TaWHfReC合金中仍然有效，其抗拉伸强度达到268 MPa。此外，在1300 ℃下，TaWHfReC合金的延伸率为23.5%，几乎是TaWHf合金的两倍。TaWHfReC合金在高温下力学性能的显著提升主要归因于位错与细小的Ta_2C析出相之间的相互作用。细小且弥散的颗粒有效抑制了位错的运动，并在高温下表现出显著的强化效果。

关键词：Ta合金；固溶强化；析出相强化；力学性能；高温

作者简介：白　润，女，1978年生，博士生，正高级工程师，西北有色金属研究院，陕西 西安 710016，电话：029-86231082，E-mail：bairunhai@163.com